Cell Cycle 13:2, 268–278; January 15, 2014; © 2014 Landes Bioscience

Hypoxia-resistant profile implies vulnerability of cancer stem cells to physiological agents, which suggests new therapeutic targets

Maria Grazia Cipolleschi[1,†], Ilaria Marzi[1,†], Roberta Santini[2], David Fredducci[1], Maria Cristina Vinci[2], Massimo D'Amico[1], Elisabetta Rovida[1], Theodora Stivarou[1], Eugenio Torre[1], Persio Dello Sbarba[1], Barbara Stecca[2], and Massimo Olivotto[1,*]

[1]Department of Biomedical, Experimental and Clinical Sciences; University of Florence; Florence, Italy; [2]Laboratory of Tumor Cell Biology; Core Research Laboratory-Istituto Toscano Tumori (CRL-ITT); Florence, Italy

[†]These authors contributed equally to this work.

Keywords: hypoxia, cancer stem cells, Krebs cycle substrates, folate metabolism, cellular redox state

We have previously shown that peculiar metabolic features of cell adaptation and survival in hypoxia imply growth restriction points that are typical of embryonic stem cells and disappear with differentiation. Here we provide evidence that such restrictions can be exploited as specific antiblastic targets by physiological factors such as pyruvate, tetrahydrofolate, and glutamine. These metabolites act as powerful cytotoxic agents on cancer stem cells (CSCs) when supplied at doses that perturb the biochemical network, sustaining the resumption of aerobic growth after the hypoxic dormant state. Experiments were performed in vivo and in vitro using CSCs obtained from various anaplastic tumors: human melanoma, leukemia, and rat hepatoma cells. Pretreatment of melanoma CSCs with pyruvate significantly reduces their self-renewal in vitro and tumorigenicity in vivo. The metabolic network underlying the cytotoxic effect of the physiological factors was thoroughly defined, principally using AH130 hepatoma, a tumor spontaneously reprogrammed to the embryonic stem stage. This network, based on a tight integration of aerobic glycolysis, cellular redox state, and folate metabolism, is centered on the cellular NADP/NADPH ratio that controls the redox pathway of folate utilization in purine synthesis. On the whole, this study indicates that pyruvate, FH_4, and glutamine display anticancer activity, because CSCs are committed to survive and maintain their stemness in hypoxia. When CSC need to differentiate and proliferate, they shift from anaerobic to aerobic status, and the few mitochondria available makes them susceptible to the injury of the above physiological factors. This vulnerability might be exploited for novel therapeutic treatments.

Introduction

A radically new approach to cancer therapy will become possible when cytotoxic agents will be selectively directed to the renewing cancer stem cells (CSCs). In other words, the new goal of therapeutic research should be to exploit crucial metabolic peculiarities in the potentially vulnerable targets of CSCs, not expressed by differentiated tissues. Little is known as yet about the metabolism of CSCs, but agreement has been reached in the characterization of some of their features, which gives grounds for hope that the new approach described below may prove to be effective.[1]

Anaplastic tumors are constantly developing successful strategies to survive in hypoxia, this being an exclusive prerogative essential for maintaining their stemness.[2] The prerogative is coupled to a biochemical marker that was discovered by Warburg as long ago as 1925, opening the way to explore cancer cell metabolism. This marker is the obligatory conversion of glucose into lactate in air, what Warburg called "aerobic glycolysis"; it is shared by embryonic tissues, but is generally absent in normal differentiated cells, which produce lactate only in anaerobiosis, a process referred to as "anaerobic glycolysis".[3] The explanation of this fundamental distinction has been the object of innumerable studies and debates, but still remains unsolved.

We approached this problem by arguing that aerobic glycolysis must imply some selective advantage for cancer cells and for embryonic cells adapted to hypoxia, when first exposed to oxygen. In fact, hypoxia adaptation requires a biochemical trim characterized by a glycolytic-oriented metabolism that counterbalances a poor mitochondrial apparatus.[4] We have previously shown that the transition from this status to that of growth and differentiation requires some O_2-dependent evolutionary steps, which lead to the amplification of the mitochondrial apparatus and the related metabolic network.[2,5,6] In these primitive steps, O_2 must be utilized through the respiratory chain to set the cellular redox state, expressed by the

*Correspondence to: Massimo Olivotto; Email: olivotto@unifi.it
Submitted: 07/09/2013; Revised: 10/31/2013; Accepted: 10/31/2013
http://dx.doi.org/10.4161/cc.27031

NADP/NADPH ratio, at values permitting crucial steps of folate utilization in the synthesis of purine ring. This synthesis is, in turn, an essential preliminary condition for the G_1/S transition of the cell cycle.[5,6] Then, in order to exit from the quiescent state, stem cells must utilize O_2 through the mitochondrial respiratory chain. In cells endowed with few mitochondria, like the hypoxia-adapted cells, this step must be protected from the saturation of the respiratory chain by pyruvate deriving from active glycolysis, necessary for ATP generation; otherwise, pyruvate itself becomes a potent cytotoxic agent and must be somehow eliminated before entering the Krebs cycle. Consistently, pyruvate addition to cancer stem cells produces a strong inhibition of transition from the anaerobic quiescent state to aerobic stimulation. In other words, the hypoxia-adapted metabolism implies a strong vulnerability to a classical physiological substrate, such as pyruvate. This observation led us to devise a series of studies aimed at exploring the biochemical background of this paradox, seeking to demonstrate the crucial role of the cellular redox state (NADP/NADPH ratio) in this event. The above metabolic trim, which characterizes cancer cells, turned out to be typical of embryonic stem cells (ESCs), which come into being in the blastula and then spread within the differentiated tissues to become adult stem cells, supporting the renewal of these tissues.[7] Such a metabolic configuration persists in the embryonic tissues and disappears with differentiation, but is restored in tumors generated in adult populations.

It seemed to us that further research in this field might reveal metabolic circuits that are preserved in cancer stem cells and could be the target of a radical antitumor therapy. At the present moment, however, we have obtained solid information about this target, showing that it represents a complex metabolic network susceptible to inhibition by physiological compounds, such as classical substrates of the Krebs cycle, pyruvate and glutamine, and the vitamin FH_4. The present study demonstrates, for the first time, the central role of the cellular redox NADP/NADPH ratio in mitotic cycle regulation in cancer stem cells.

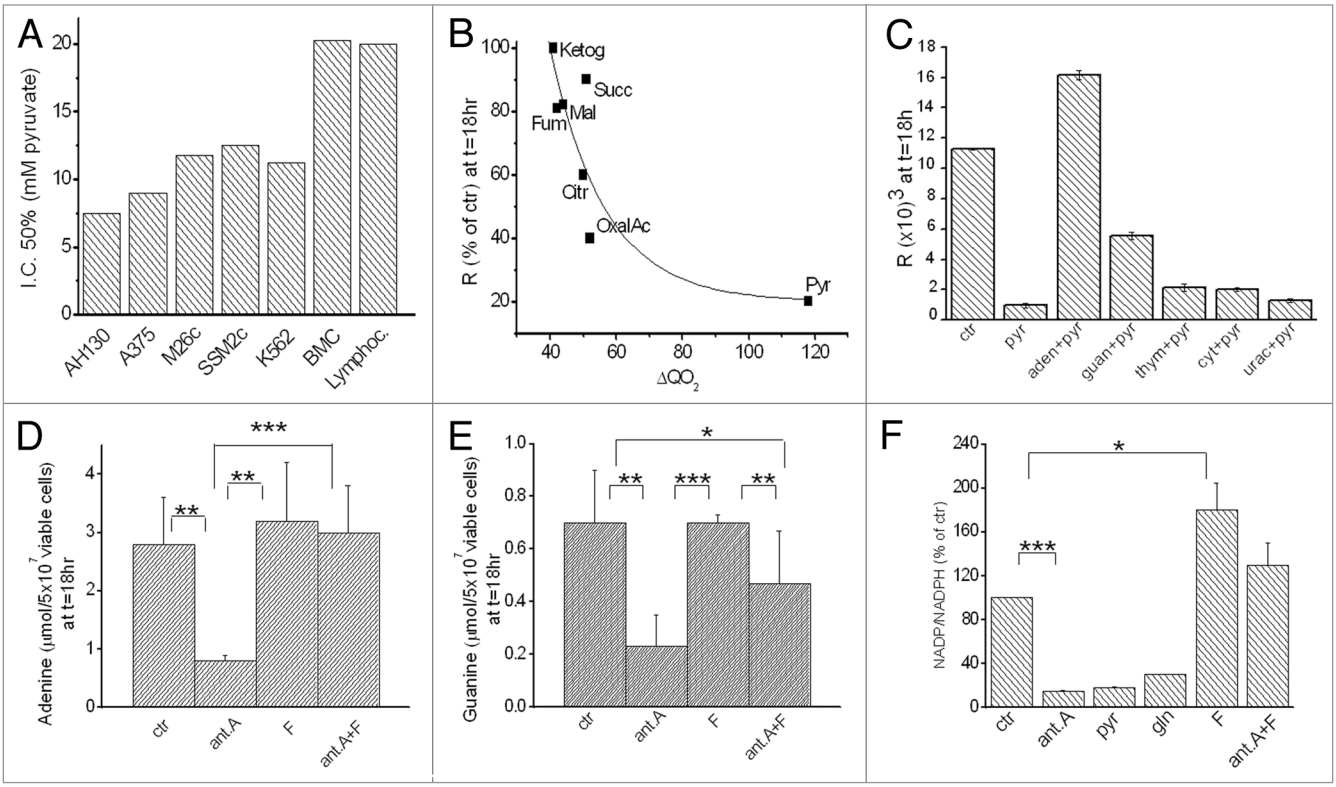

Figure 1. The role of cellular redox-state in the cytotoxic activity of physiological agents: the involvement of purine and folate metabolism. (**A**) The sensitivity of various cancer and normal stem cell populations to the cytotoxic activity of pyruvate. Values are expressed as IC_{50} of cell growth in the presence of varying concentrations of the substrate. (**B**) The inhibition of cell recruitment into S of AH130 cells by the Krebs cycle substrates as a function of the corresponding rate of oxygen consumption. Oxygen consumption (ΔQO_2) is expressed as μl of O_2 per mg of dry weight per hour. Ketog, α-ketoglutarate; Succ, Succinate; Mal, Malate; Fum, Fumarate; Citr, Citrate; OxalAc, Oxalacetate; Pyr, Pyruvate. All substrates are used at [10 mM]. R = rate of ^{14}C-Thymidine incorporation into DNA per 90min per 10^6 viable cells at t = 18 h of incubation in air. Values are expressed as % of control. (**C**) Effects of purine and pyrimidines on pyruvate inhibition of AH130 cell recruitment into S. Additions: pyr = 10 mM pyruvate; ade, adenine; guan, guanine; thym, thymidine; cyt, cytosine; urac, uracile. All bases are used at [0.5 mM]. All additions were performed at time 0. Values are means ± SEM of 3 experiments. (**D**) The antimycin An inhibition of adenine pool and its removal by folate in AH130 cells. Values are expressed as nmol/5 × 10^7 viable cells at t = 18 h of incubation in air and are means ± SEM of 6 experiments. Ant A (6×10^{-6}M), F (100 μmol) were added at t = 0. ant A, antimycin A; F, folate. (**E**) The antimycin A inhibition of guanine pool and its removal by folate in AH130 cells. Values are expressed as nmol/5 × 10^7 viable cells at t = 18h of incubation in air and are means ± SEM of 3 experiments. Ant A and F were added at t = 0. (**F**) The effects of various treatments on the intracellular NADP/NADPH ratio in AH130 cells. NADP and NADPH were estimated by HPLC technique as reported in "Materials and Methods" and are expressed as percentage of control at t = 18 h of incubation in air, and are means ± SEM of five experiments. gln, glutamine (5 mM). $^{**}P < 0.02$; $^{***}P < 0.001$.

Results

A preliminary screening performed on cell populations of varying histogenesis and tumorigenicity displayed a higher sensitivity to pyruvate in cancer cell lines as compared with normal cell populations (**Fig. 1A**). To be more precise, the IC_{50} was 7.5 mM for the highly anaplastic hepatoma ascites AH130, and about 10 mM for the 3 human melanoma lines, A375, M26c, and SSM2c. A similar sensitivity was displayed by the K562 line, composed of undifferentiated blast cells.[8,9] By contrast, 2 normal stem populations, namely, bone marrow hematopoietic cells (BMC) and lymphocytes, proved to be much less sensitive. Taken as a whole, these data indicate that pyruvate sensitivity reflects a metabolic trim, which, without being limited to cancer cells, is greatly intensified in aggressive malignancies.

The AH130 hepatoma model

The AH130 tumor closely mirrors the cancer profile at embryonic stages of de-differentiation and hypoxia adaptation.[2,6] It was generated in liver by the carcinogen *o-aminoazotoluene*, which bound to and abolished the p53 protein, producing a

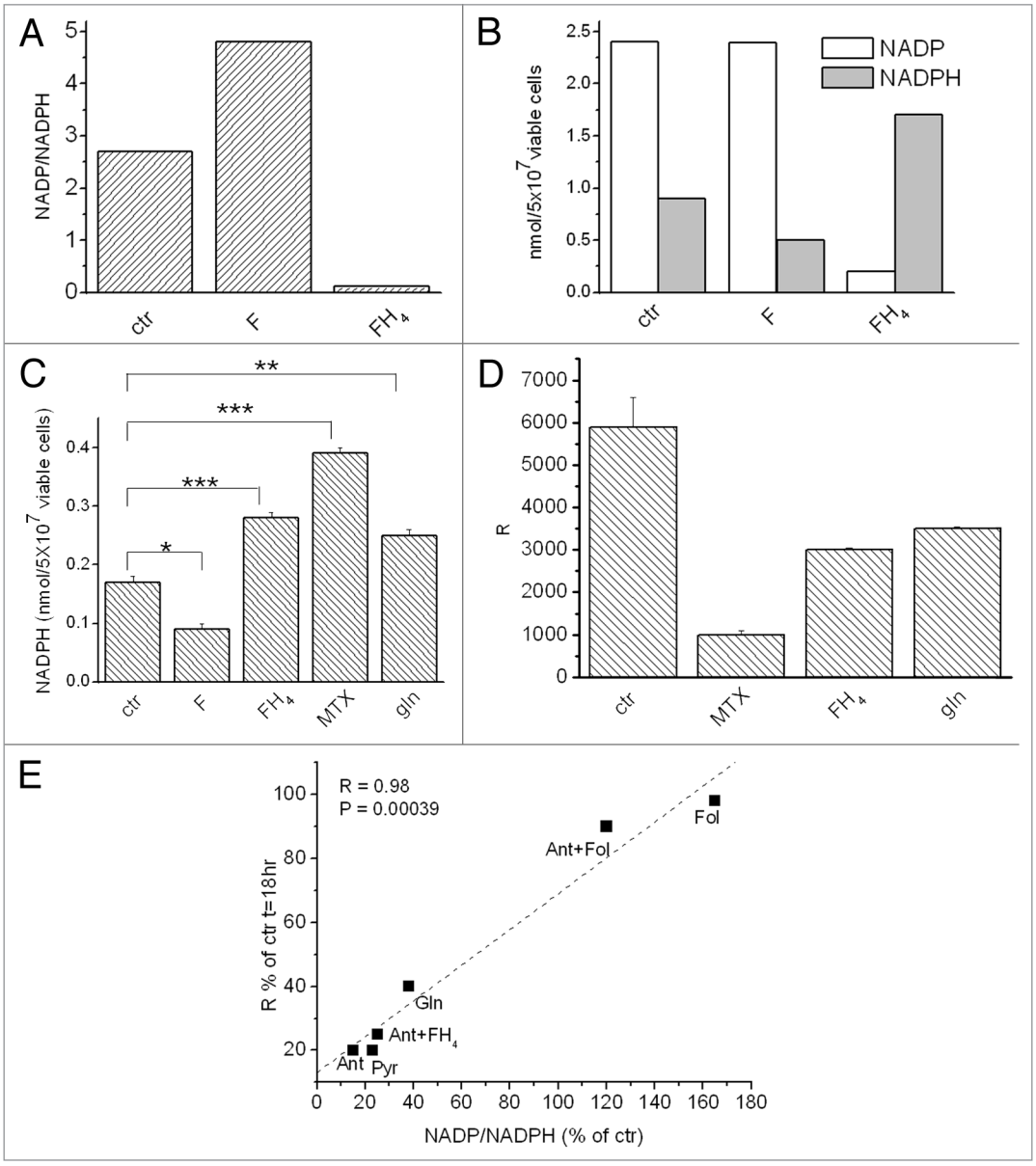

Figure 2. The central role of the NADP/NADPH ratio in the control of ascites cell recruitment into S. The paradoxical effect of FH_4 and its similarity to that of MTX. (**A**) The opposite effect of F and FH_4 on the NADP/NADPH ratio. The ratio was determined at 18 h of incubation in air. Additions were performed at t = 0. F and FH_4 = 100 μM. (**B**) The effect of F and FH_4 on the NADP or NADPH intracellular concentration. Note that in the presence of folate, NADP concentration is much higher that of NADPH, while FH_4 inverts this ratio. Values are expressed as nmol/5 × 10^7 viable cells at t = 18 h of incubation in air. (**C**) The effects of F, FH_4, MTX (10^{-6} M) and gln on the NADPH intracellular concentration. Values are expressed as nmol/5 × 10^7 viable cells at t = 18 h of incubation in air and are means ± SEM of 3 experiments. (**D**) The effects of FH_4, MTX and gln on AH130 cell recruitment into S (R). Values are means ± SEM of 3 experiments. (**E**) The correlation between AH130 cell recruitment into S and the NADP/NADPH under various conditions. Correlation index, R = 0.98. *P < 0.05; **P < 0.02; ***P < 0.001.

genomic instability that promoted both an intense neoplastic progression and a significant reprogramming to embryonic staminality. This reprogramming was demonstrated by the expression of embryonic transcription factors (ETFs), such as Nanog, Klf4, and c-Myc, in the entire cell population.[2] When injected into peritoneal cavity of a new host rat, this stem population grows with an unlimited capacity for self-renewal for as long as oxygen is available. At more advanced stages, when the intraperitoneal pO_2 falls to ~0, almost 100% of the cells survive, blocked in G_0/G_1; when transferred into aerobic culture, the entire population is synchronously recruited into S.[2] Overall, this population proved to be a unique source of reprogrammed cancer stem cells obtainable in such a quantity (billions) naturally synchronized by hypoxia and synchronously recruited into S upon exposure to normoxia. In this model we were able to demonstrate that the G_1/S transition is abolished by antimycin A, a powerful inhibitor of the electron transport to oxygen through the mitochondrial respiratory chain,[6,10] and it was also possible to bring about a detailed quantitative study of the role of aerobic glycolysis in prevention of the cell cycle inhibition by pyruvate. We also showed that varying levels of inhibition were obtained with the addition of classical substrates of the Krebs cycle, first and foremost pyruvate, this being the initial observation that led to the research reported in this paper.

The inhibitory activity of the Krebs cycle substrates is a function of their oxidation rate through the respiratory chain

In **Figure 1B**, cell recruitment into S, measured by the rate of incorporation of ^{14}C-thymidine into DNA at 18 h of incubation in air (R), is reported as a function of the oxygen consumption (ΔQO_2)[11] produced by the respective substrates. As shown, this recruitment is inhibited as a strict function of ΔQO_2, which suggests that the oxidation of substrates governs growth inhibition, so that at 10 mM, pyruvate produced the same level (80%) of inhibition as antimycin A.[5,6] This paradox suggested that an excess of oxidizable substrates saturates the respiratory chain, at the expense of some redox step, limiting the activation of the cell cycle.[2,6] As demonstrated below, this step was individuated in a redox reaction of a complex metabolic network responsible for the synthesis of the purine ring.

The regulation of purine pools by the cellular redox state: The role of the NADP/NADPH ratio and its dependence on folate

The central role of a cellular redox pathway in purine synthesis was demonstrated by the following results: (1) Pyruvate inhibition of cell recruitment was totally removed by the addition of 0.5 mM adenine and reduced by half adding guanine, while pyrimidines (thymine, cytosine, uracil) were ineffective (**Fig. 1C**). (2) Antimycin A produced a 70% reduction of the intracellular adenine and guanine pools, measured by HPLC analysis at 18 h of incubation in air (**Fig. 1D and E**): these results demonstrate that the synthesis of these bases requires a respiration-dependent oxidative step. (3) The addition of folate removed antimycin A inhibition of adenine and guanine pools: this leads us to ascribe the redox limiting step of folate utilization in purine synthesis to the NADP/NADPH ratio, which governs the generation of the essential precursor methenyl-tetrahydrofolate ($CH\text{-}FH_4$) from methylentetrahydrofolate ($CH_2\text{-}FH_4$), mediated by methylentetrahydrofolate dehydrogenase ($CH_2\text{-}FH_4DH$) (**Fig. 6**). (4) The mitochondrial respiratory chain gears the cellular NADP/NAPH ratio: this was made evident by the experiments reported in **Figure 1F**, showing that antimycin A, as well as pyruvate, produces a 90% fall of this ratio. Such inhibition is totally removed by folate, which doubles the NADP/NAPH ratio of the control.

The tumor inhibition by tetrahydrofolate (FH_4)

Another unpredictable feature of cancer stem cells emerged from the data reported in **Figure 2**, showing that the addition of folate and FH_4 has opposite effects on the NADP/NADPH ratio, which was strongly enhanced by folate and drastically diminished by FH_4 (**Fig. 2A**). It is important to note that this diminution was accounted for by the NADPH increase at the expense of folate (**Fig. 2B**). These effects of FH_4 closely mimic those of Metatrexate, the powerful inhibitor of the DHFR, producing: (1) a comparable increase of the cellular NADPH levels (**Fig. 2C**); and (2) the inhibition of cell recruitment into S, as measured by the thymidine incorporation rate into DNA (**Fig. 2D**). Keeping in mind that FH_4 is the biologically active derivative of folates, taken in their totality, these results configure another apparent paradox emerging from this study.

The tumor inhibition by glutamine

It has been recently demonstrated that glutamine, an essential factor in culture media,[12] contributes to the generation of NADPH necessary to the reductive syntheses through the glutaminolytic pathway.[13,14] However, the data reported above demonstrate that the increment of NADPH inhibits cancer stem cell recruitment into S. As shown in **Figure 1F**, the addition of 5 mM glutamine consistently brought about a decrease in the NADP/NADPH ratio similar to that produced by antimycin A and pyruvate, due to the increase in NADPH (**Fig. 2C**). This reduction is accompanied by 50% inhibition of cell recruitment (**Fig. 2D**). These results reveal another paradoxical response of cancer stem cells to physiological agents, in keeping with the crucial role of the NADP/NADPH ratio in cell cycle activation.

The central role of the NADP/NADPH ratio in cancer cell cycle activation

On the evidence of the data summarized in **Figure 2E**, the NADP/NADPH ratio appears to be the key growth regulator of cancers of different histogenesis, whatever the factor added in culture, including antimycin A, pyruvate, and folate, and whatever the source of NADPH, including glutamine, through the glutaminolytic pathway.[13,14]

The melanoma model

We employed the human melanoma cell line A375 and 2 metastatic melanomas obtained from patients (SSM2c and M26c), using a protocol[15] suitable to estimate the effects of physiological cytotoxic agents or MTX on self-renewal of these cell populations. These cells were transferred into flasks containing a medium supporting primary spheres generation from single cells. Sphere formation is considered a selection method that enriches for cancer stem cells. These spheres were dissociated and treated with various agents for 5 days up to the formation of secondary spheres, as illustrated in **Figure 3A–E**

(A375), **Figure 3F–J** (SSM2c), and **Figure 3K–O** (M26c). Folate treatment of A375 cells (**Fig. 3B**) did not cause any significant effect on the sphere production; on the contrary FH_4 and pyruvate (**Fig. 3C and D**) practically abolished sphere formation to the same extent of MTX (**Fig. 3E**). The abolition of spheres was accompanied by extensive apoptotic cell loss, as shown in **Fig. 3P and Q** by the strong positivity to cleaved caspase 3. Similar results were obtained for the 2 metastatic melanomas, SSM2c and M26c (**Fig. 3F–J** and **K–O**, respectively). These data indicate that the physiological agents FH_4 and pyruvate exert a strong cytotoxic effect on melanoma cells, similar to that of MTX, drastically interfering with sphere formation. The effects of these compounds on cell number in culture are shown in **Figure 4A**, which reports the total number of cells obtained by the dissociation of secondary spheres at the end of treatment. This number was strongly reduced by each treatment in all 3 lines, with a minor sensitivity in SSM2c to FH_4 200 μM and some degree of resistance to MTX by the A375 cells. Overall, the highest level of sensitivity displayed by the 3 lines was that to the treatment with pyruvate.

Crucial information was obtained in these experiments by measuring the self-renewal of cells dissociated from secondary spheres. To this purpose, these cells were plated at limiting dilution (1 cell/μl) up to spheres formation (tertiary spheres) in the absence of any treatment. The number of these spheres is reported in **Figure 4B–D**. As shown, folate was ineffective, whereas pyruvate, FH_4, and MTX strongly reduced the production of tertiary spheres. A comparison among the 3 lines indicates that the response is substantially similar, except for the striking sensitivity of A375 cells to 200 μM FH_4. These results indicate that the cytotoxicity of the tested physiological agents not only reduces the melanoma cell generation, but it is also

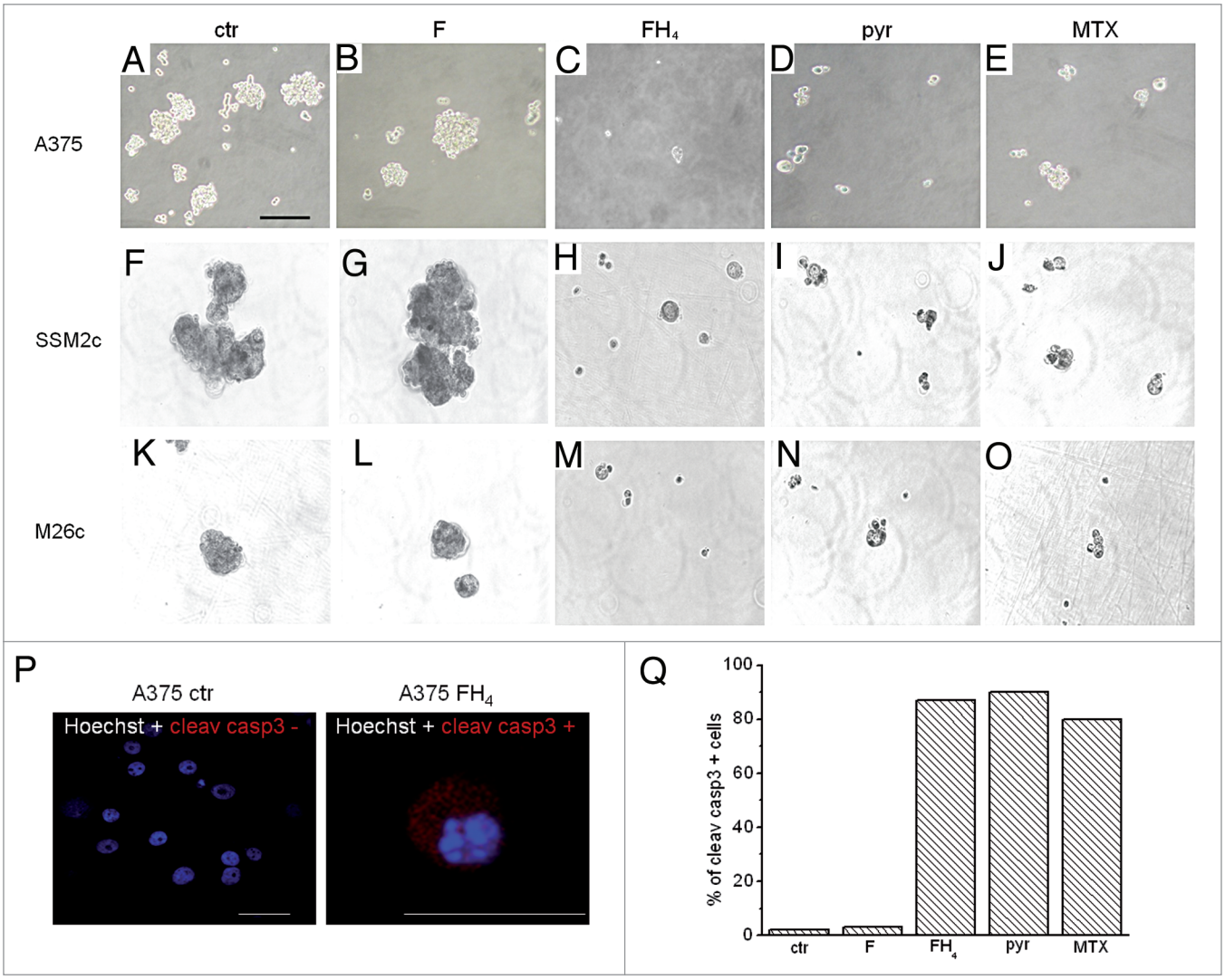

Figure 3. The cytotoxic effects of physiological agents on melanoma stem cells. (**A–O**) Effects of various treatments on sphere formation from A375 (**A–E**), SSM2c (**F–J**), and M26c cells (**K–O**). f = 100 μM, FH_4 = 100 μM, pyr = 20 mM, MTX = 10^{-6}M. (**P**) The apoptotic death of A375 melanoma cells induced by FH_4 treatment, as revealed by anti-cleaved caspase3 antibody immunostaining. Note the fragmented apoptotic nucleus (Hoechst) and the intense expression of the caspase in the cytoplasm after FH_4 treatment. Scale bar = 100 μm. (**Q**) Percentage of Cleav caspase 3-positive cells after treatment with cytotoxic physiological agents.

memorized, influencing the self-renewal ability by the further sphere generation after the agent removal. This conclusion is most relevant for the interpretation of the action mechanism of the cytotoxicity. This mechanism cannot be attributed now exclusively to a direct metabolic effect, but it is also brought about through a memorization influence (see "Discussion"). This "memorization process" was confirmed by the in vivo experiments reported below.

In vitro treatment with pyruvate reduces tumorigenicity of melanoma cancer stem cells: The cytotoxic nature of pyruvate

The memorization was confirmed by the in vivo experiments reported in **Figure 5**. An aliquot of A375 dissociated cells from primary spheres was split in 2 cultures, which were incubated for 1 wk either in presence of 20 mM pyruvate or PBS. At the end of this incubation, 10^3 viable pyruvate- or PBS-treated cells were injected subcutaneously into nude mice to test their tumorigenicity. As shown in **Figure 5A**, pyruvate pretreatment caused an inhibition of tumor growth, determining a remarkable reduction of tumor number and size (**Fig. 5B**). Histological examination of xenograft cross sections showed that the central parts of tumors derived from both PBS-treated and pyruvate-treated CSC were necrotic, consistent with the progressive pO_2 decrease from the periphery to the center of the tumor. The periphery of tumors derived from PBS-treated melanoma cancer stem cells (**Fig. 5C**, upper pictures) is thicker and more preserved than that of pyruvate-treated melanoma CSC (**Fig. 5D**, lower pictures); moreover, in the latter, cells appear visibly necrotic. This implies that, unlike the apoptotic effect of pyruvate pretreatment on melanoma cells in vitro (**Fig. 3P**), the necrotic effect produced in vivo was evidently brought about without exploiting the ATP-dependent apoptotic program of cell death. It is conceivable that the hypoxic environment of the tumor in vivo is responsible for this reinforced cytotoxicity of pyruvate.

Discussion

This study demonstrates that the metabolic configuration peculiar to cancer stem cells is responsible for both the successful strategy of neoplastic development in order to ensure survival in hostile environments, and the reason for its vulnerability to crucial physiological agents.

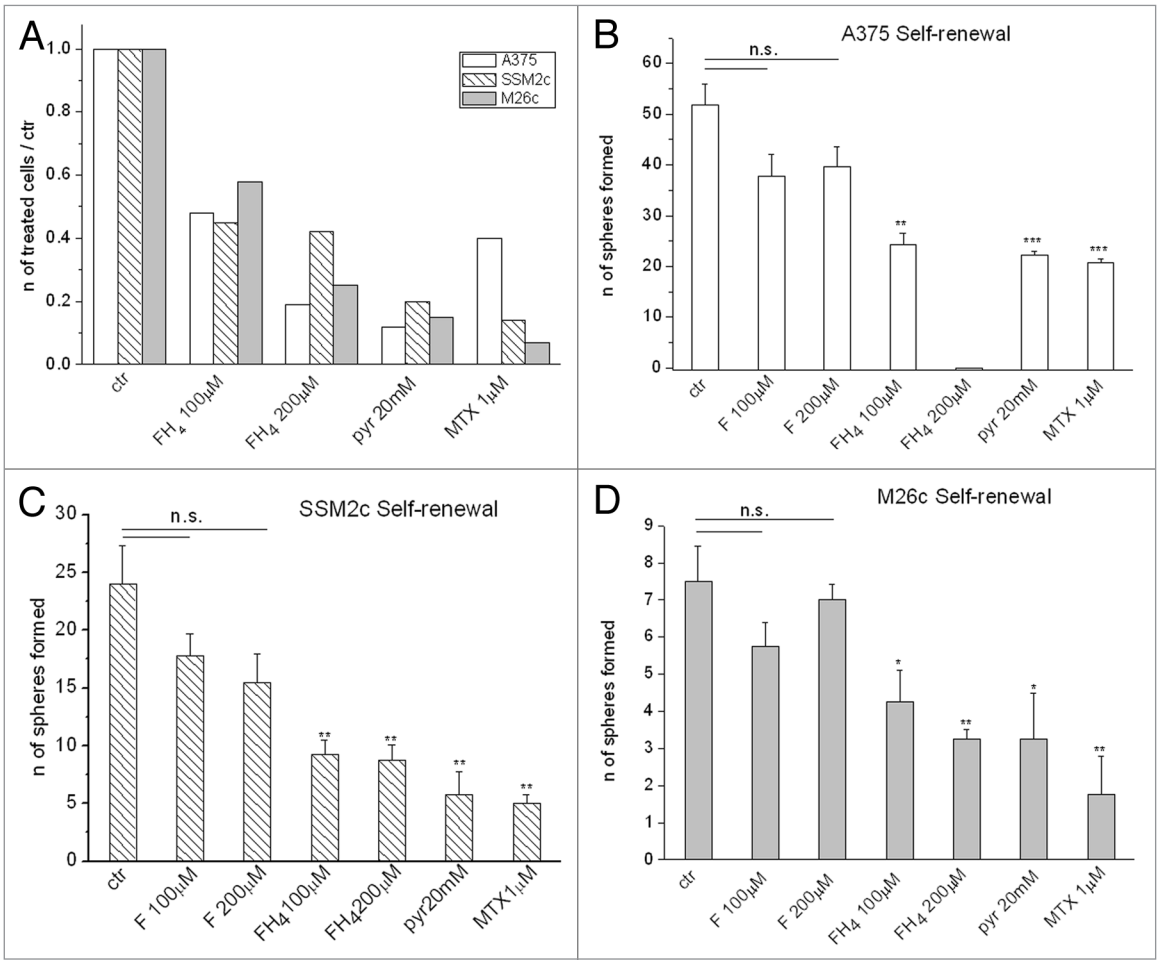

Figure 4. The inhibition of self-renewal by various agents in melanoma stem cells. (**A**) The effects of treatments with various agents on the number of cell dissociated from secondary spheres in the 3 melanoma cell lines. (**B–D**) The effects of treatments on self-renewal in A375, SSM2c, and M26c cells. Bars represent the number of spheres generated in the absence of treatments by dissociated cells obtained from the secondary spheres. Values are means ± SEM of 3 experiments. *$P < 0.05$; **$P < 0.02$; ***$P < 0.001$.

The anticancer cytotoxicity displayed by pyruvate, FH_4, and glutamine derives from the metabolic organization specific to stem cells committed to survive and maintain their stemness in hypoxia. This organization is constantly configured in highly anaplastic tumor cells, revealing unsuspected vulnerabilities of cancer. As summarized in the diagram in **Figure 6**, despite their different chemical structure and metabolic role, the 3 substances produced remarkably similar effects by means of a remarkably similar mechanism of a kind that could not have been predicted. What happens is that all 3 are similarly targeted to the metabolic checkpoint, which regulates the activation of the stem-cell cycle at the G_1/S transition. The following detailed definition of the metabolic sequence altering this checkpoint was allowed in the AH130 model, showing that the final target of the cytotoxic agents on embryonic cancer cells is the redox NADP/NADPH ratio. This ratio governs folate utilization in the amplification of purine pools, which is necessary to start DNA neosynthesis in hypoxia-starved stem cells (**Fig. 6A**). The crucial step in this process is the NADP-dependent oxidation of CH_2-FH_4 to CH-FH_4, catalyzed by CH_2-FH_4DH.[14] Consequently, any reductive shift of the NADP/NADPH ratio tends to impair cell recruitment into S. The addition of pyruvate, as well as FH_4 and glutamine, produces a drastic shift of the ratio, accounting for a proportional inhibition of the recruitment.

Pyruvate decreases the NADP/NADPH ratio by saturating the respiratory chain and, thus, mimics the blockade by antimycin A. Such interpretation is confirmed by the removal of this blockade by folate, which abolishes this decrease (**Figs. 1 and 2**).This fact rules out that the cytotoxicity of pyruvate might be mediated by some defect of the activity of pyruvate dehydrogenase (PDH)

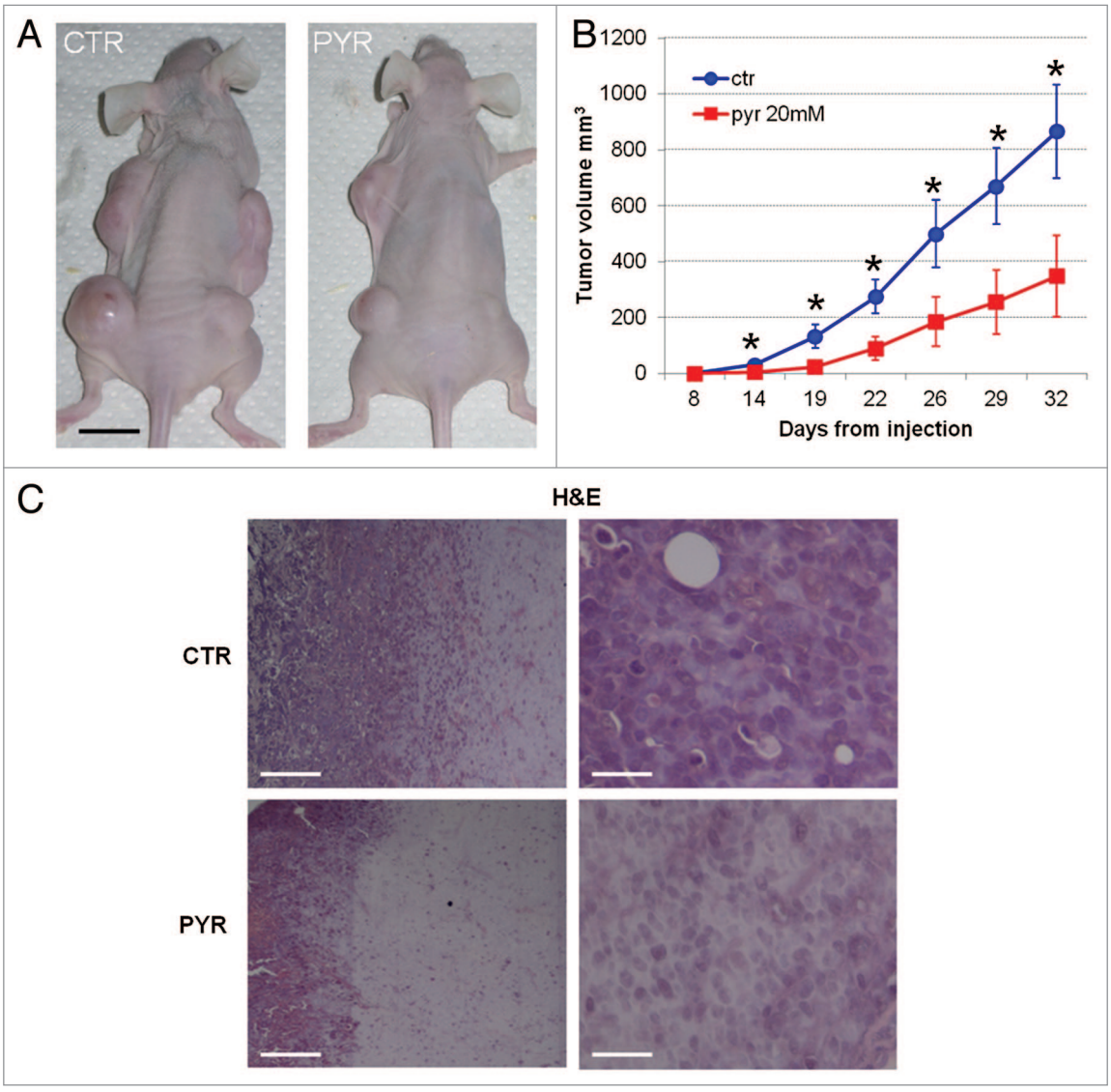

Figure 5. Pre-treatment of A375 melanoma cells with pyruvate in vitro reduces tumor growth in vivo. (**A**) The inhibitory effect of pyruvate pre-treatment on melanoma growth in vivo. A375 melanoma spheres were treated and injected in athymic mice as reported in "Materials and Methods", and tumor development followed up to 32 d from injection. Scale bar = 10 mm. (**B**) Quantification of tumor volume. Values represent the averages of tumors developed at various times and expressed as mean ± SEM (n = 12, each). (**C**) Histological sections of tumors derived from PBS- (upper pictures) and pyruvate-treated melanoma stem cells (lower pictures) counterstained with Hematoxylin and Eosin (H&E). Scale bar right pictures = 100 μm, left pictures = 500 μm.

as well as that of the regulatory phosphatase and kinase. This is an important point with regard to our interpretation, in view of the fact that PDH, a gatekeeper linking glycolysis to oxidative metabolism, acts a potent barrier against malignant transformation (Kaplon et al., 2013).[16] Both blockade and saturation impair the shuttle mechanisms, which transport the reducing equivalents generated by the cytosolic dehydrogenases into mitochondria, to be disposed of by the respiratory chain (**Fig. 6C**).[17]

The cytotoxicity of FH_4 is mediated by the restriction of the reaction F + NADPH® FH_4 + NADP. This restriction should account for the reductive shift of the NADP/NADPH ratio, demonstrated by our experiments, down to values incompatible with the purine pool amplification. All in all, an excess of FH_4 behaves like an inhibitor of DHFR; this interpretation is supported by the demonstration that a powerful inhibitor of this enzyme, MTX, produces the same increment of cellular NADPH as that brought about by FH_4, together with a similar inhibition of cell recruitment into S (**Fig. 2**).

The central role of the NADP/NADPH ratio in the pathogenesis of the cytotoxicity of physiological agents is further confirmed by the inhibitory effect of glutamine, whose addition determines a reductive shift of the ratio through the glutaminolytic pathway.[12,13]

To summarize thus far: the common target of the cytotoxic activity of physiological agents is purine neosynthesis, through the alteration of the cellular redox state expressed by the cytosolic NADP/NADPH ratio (**Fig. 6**).

An alternative mechanism underlying the necrotic or apoptotic cytotoxicity of the agents examined in this study is the persistence of this activity in vitro and in vivo long after this substrate has been removed or exhausted (**Figs. 3–5**). This long-term effect, shared by pyruvate, FH_4, and MTX, is traceable to a fixable, epigenetic influence on ETFs, proved to regulate the activation

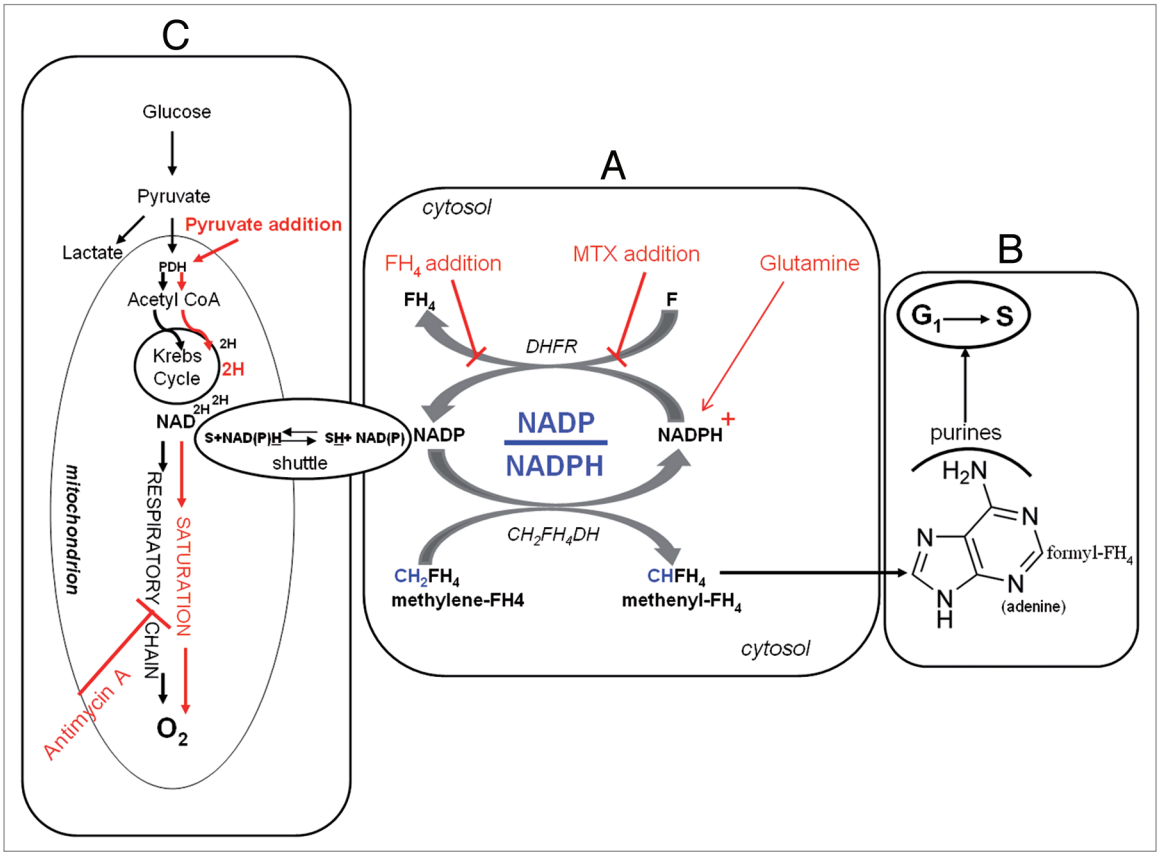

Figure 6. The metabolic network which regulates the cell cycle activation at the O_2-dependent G_1/S transition. The core of the network is the cellular redox-state expressed by the cytosolic NADP/NADPH ratio. This ratio (**A**) regulates the transfer of reducing equivalents (H) from the methylentetrahydrofolate (CH_2-FH_4) to methenyltrahydrofolate (CH-FH_4), a crucial NADP-dependent reaction generating NADPH. This is a limiting step of the synthesis of purine ring (**B**), required for the amplification of purine pools indispensable for the G_1–S transition. A fundamental role in the regulation of the NADP/NADPH ratio is played by folate, whose reduction to FH_4 by the dehydrofolic reductase (DHFR) generates NADP (**A**). The addition of an excess of the reaction product, FH_4, can impair the DHFR activity, leading to an increment of NADPH, with the consequent reductive shift of the NADP/NADPH ratio and the inhibition of the G_1/S transition. Consistently, FH_4 mimics the effects of MTX, a powerful inhibitor of DHFR (**A**), incrementing the NADPH levels and inhibiting cell recruitment into S. Whatever the mechanism incrementing the cytosolic NADPH, including an excess of glutamine through the glutaminolytic pathway (**A**), has an inhibitory effect, unless it is removed by the shuttle mechanisms, which discharge the cytosolic reducing equivalents onto the mitochondrial respiratory chain. This role of the shuttles accounts for the fact that the activity of the chain is crucial for the G_1/S transition, which is impaired by a specific inhibitor like antimycin A (**C**). A similar inhibition can be performed whenever the chain, although not inhibited, it is saturated by reducing equivalents produced by oxidizable substrates of the Krebs cycle, mostly pyruvate.

of the stem-cell cycle. Actually, we demonstrated that pyruvate modifies the assembly of the complex transcriptional loop of *Nanog*, *Klf4*, and *c-Myc*, which governs the pO_2-dependent cycle activation of ascites hepatoma stem cells that we described in our previous work.[2] In this loop, *Nanog* and *Klf4* antithetically control the expression of *c-Myc* and, hence, the activation of the cell cycle. The addition of pyruvate shifted the *Nanog/Klf4* ratio to values that suppress the activation of *c-Myc*, thus contributing to the impairment of the G_1/S transition. This mechanism reinforces the cytotoxic activity of pyruvate. The essential feature of this model lies on a poor mitochondrial cellular equipment, whose saturation by glycolytic reducing equivalents is prevented by the aerobic pyruvate conversion to lactate. This effect is produced in normal embryonic stem cells and in highly anaplastic tumors, while it is not produced in differentiated cells, which are normally endowed with an expanded mitochondrial apparatus.

As regards the hypothetical use of these physiological agents in anticancer therapy, it should be recalled that their cytotoxicity is only operative in the presence of a poor mitochondrial apparatus, typical of hypoxia-adapted embryonic stem cells. This might, per se, represent a substantial advantage with respect to the current chemo- and radiotherapies, which are ineffective on this compartment. It must be conceded immediately that there is a possible limit to this approach, deriving from the fact that the cytotoxicity of these factors might produce a negative effect on normal stem cells endowed with a scanty mitochondrial equipment, such as adult, hematopoietic stem cells.[18-23] Nevertheless, our own preliminary experiments showed that the sensitivity of these cell types is at least 4 times lower than that displayed by the malignant cancer populations tested so far, and this would provide a reasonable therapeutic index. In addition, the memorization of the mechanism mediating the cytotoxicity might allow the accumulation of this effect in the target embryonic cancer stem cells through a repetitive drug supply, obviating the exhaustive metabolization operated by adult tissues.

Materials and Methods

Tumor transplantation and cell transfer in culture

AH130 ascites hepatoma was obtained by T Yoshida[24] by treating Wistar rats with the carcinogen *o*-aminoazotoluene. After serial transplantations in the rat peritoneal cavity, the tumor became composed of isolated spheroidal cells, fed by the ascites fluid exuded from the peritoneal vessels. These cells displayed a totally undifferentiated phenotype, with a high nucleus/cytoplasm ratio, few mitochondria, and unlimited self-renewal. Maintaining the tumor in vivo, treatments in vitro, and the standard procedure for labeling DNA were performed essentially as previously described.[2,5]

Measurement of oxygen consumption

Oxygen consumption (ΔQO_2) of ascites cells was measured, as reported by Del Monte[11] by Warburg direct method.[25]

HPLC measurements

The organic extracts were obtained from AH130 cells (5×10^7) with 75% acetonitrile ultrapure plus 25% 10 mM KH_2PO_4 at pH 7.4.[26] The extracts were completely dehydrated and suspended in 20 µl of A running buffer (see below). The HPLC apparatus consisted of a Perkin Elmer Series 200 binary pump system, equipped with a UV/VIS detector. Data were acquired and analyzed by a PC using the Total Chrom Workstation. The separation of purines, pyrimidines, NAD, NADH, NADP, and NADPH was performed using a Gemini-NX 5-µm particle size C18 110A, 250 × 4.60-mm column (Phenomenex), which was provided with its own guard column (Guard Cartridge System). Freshly prepared standard mixtures (Sigma Aldrich), with known concentrations were assayed by ion-pairing HPLC for the separation of adenine, guanine, thymine, cytosine, uracil, NAD, NADH, NADP, and NADPH, and they were detected at a wavelength of 260 nm. The mobile phase was composed by an A buffer (KH_2PO_4 10 mM, methanol 0.125%, tetrabutylammonium hydroxide 12 mM) obtained as a 55% water solution from Nova Chimica and a B buffer (KH_2PO_4 100 mM, methanol 30%, Sigma-Aldrich), tetrabutylammonium hydroxide 2.8 mM. All bases were detected with an isocratic run with A buffer in 10 min, whereas NAD, NADH, NADP, and NADPH were detected with a step gradient from 100% A to 95% B in 40 min: both runs were performed at the flow rate of 1.2 ml/min. The volume of sample injected was, in all cases, 20 µl.

K562 cell line

Thirty × 10^3 K562 cells/ml were plated in RPMI-1640 medium supplemented with 10% fetal bovine serum, 50 U penicillin, and 50 µg streptomycin/ml (EuroClone).[8,9] Incubation was performed at 37 °C in a 95% air, 5% CO_2 atmosphere in a humidified incubator.[27] Bone marrow cells and lymphocytes were obtained and treated as previously described.[28,29]

Human melanoma cells, tumor spheres, and in vitro self-renewal assay

Human melanoma cells A375 were from ATCC, whereas patient-derived SSM2c and M26c were obtained after approved protocol by the Ethic Committee as already described.[15] For adherent culture, cells were grown in DMEM with fetal bovine serum (FBS). For melanoma sphere culture, cells were seeded at a concentration of 5 cells/µl in DMEM-F12 serum-free medium with N_2 supplement, insulin (20 µg/ml), EGF (10 ng/ml), FGF-2 (10 ng/ml) (all from Invitrogen), or in human embryonic stem cell medium (hESCM), as previously described.[14] Treatments with PBS or physiological agents (pyruvate, folate, thetrahydrofolate) and MTX were performed for 5 d in DMEM/F12 or hESCM medium, lowering EGF and bFGF concentration to 2 ng/ml. After treatment, spheres were dissociated, counted, and plated for self-renewal assay (in 96-well plates at one cell per well or in 12-well plates at one cell per microliter) without the drugs. After 1 wk, spheres were counted. All the experiments were performed in triplicate and were repeated at least 3 times.

Immunofluorescence

Immunofluorescence for cells in suspension (cytocentrifuged at 800 rpm for 15 min at 4 °C) was done essentially as previously described in Marzi et al.[2] Cell cultures were fixed in 3.7% formaldehyde in PBS for 20 min at 4 °C and then incubated with

Hoechst at room temperature for 10 min to stain cell nuclei. A375 cell population was tested for rabbit anti-cleaved caspase3, 1:200 (Cell Signaling Technology Boston). After washing with PBST, the cell cultures were incubated with secondary antibody, anti-rabbit Cy3 conjugated (Chemicon) (1:800 dilution in PBST/3% BSA) for 1 h at room temperature.

Xenografts

In vivo experiments were conducted in accordance with National Guidelines and approved by Ethical Committee of Animal Welfare Office of Italian Health Ministry. A375 spheres treated with PBS or 20 mM pyruvate for 7 d were dissociated, resuspended in PBS, and mixed with DMEM/Matrigel in a 1:1 ratio, and inoculated subcutaneously in adult female athymic nude mouse (Foxn1 nu/nu) (1000 cells/injection). Animals were monitored daily, subcutaneous tumor size was measured every 2–3 d by a caliper, and tumor volumes were calculated using the formula $V = W^2 \times L \times 0.5$, where W and L are tumor width and length, respectively.[15] Mice were euthanized 32 d after implantation. For histological analysis, xenografts were fixed in 4% formaldehyde, paraffin-embedded, cut to 5-μm sections, and stained with hematoxylin and eosin (H&E).

Drugs and chemicals

All the substances tested were purchased from Sigma Aldrich and added at time 0 at the concentration indicated in the legends.

Statistical analysis

Significance levels were calculated with a Student *t* test: $^{*}P < 0.05$; $^{**}P < 0.02$; $^{***}P < 0.005$.

Disclosure of Potential Conflicts of Interest

No potential conflicts of interest were disclosed.

Acknowledgments

We are grateful Prof P Boyde, University of Cambridge, UK, for his help in the revision of the manuscript. This paper is dedicated to the memory of Prof E Ciaranfi and Prof A Fonnesu, who directly from Warburg's and Krebs's laboratories transmitted to us the intellectual commitment and the rigorous experimental skill required for studying cancer development.

Grant Support

This work was supported by grants from Ente Cassa di Risparmio di Firenze, Istituto Toscano Tumori (ITT), Associazione Italiana per la Ricerca sul Cancro (AIRC), Regione Toscana, and Ministero della Salute.

Financial Support

Maria Grazia Cipolleschi, Ilaria Marzi, David Fredducci, Massimo D'Amico, Theodora Stivarou, Eugenio Torre, and Massimo Olivotto are supported by Ente Cassa di Risparmio di Firenze (grants n. 2010.1055, 2011.0335); Roberta Santini, Maria Cristina Vinci, and Barbara Stecca are supported by Associazione Italiana per la Ricerca sul Cancro (AIRC) (grant n. 9566); Elisabetta Rovida and Persio Dello Sbarba are supported by Istituto Toscano Tumori (ITT), AIRC, Istituto Superiore di Sanità (Grant n CS64), and Ministero della Salute (grant n. RF-TOS-2008-1163728).

References

1. Simsek T, Kocabas F, Zheng J, Deberardinis RJ, Mahmoud AI, Olson EN, Schneider JW, Zhang CC, Sadek HA. The distinct metabolic profile of hematopoietic stem cells reflects their location in a hypoxic niche. Cell Stem Cell 2010; 7:380-90; PMID:20804973; http://dx.doi.org/10.1016/j.stem.2010.07.011
2. Marzi I, Cipolleschi MG, D'Amico M, Stivarou T, Rovida E, Vinci MC, Pandolfi S, Dello Sbarba P, Stecca B, Olivotto M. The involvement of a Nanog, Klf4 and c-Myc transcriptional circuitry in the intertwining between neoplastic progression and reprogramming. Cell Cycle 2013; 12:353-64; PMID:23287475; http://dx.doi.org/10.4161/cc.23200
3. Warburg O. On respiratory impairment in cancer cells. Science 1956; 124:269-70; PMID:13351639
4. Simsek T, Kocabas F, Zheng J, Deberardinis RJ, Mahmoud AI, Olson EN, Schneider JW, Zhang CC, Sadek HA. The distinct metabolic profile of hematopoietic stem cells reflects their location in a hypoxic niche. Cell Stem Cell 2010; 7:380-90; PMID:20804973; http://dx.doi.org/10.1016/j.stem.2010.07.011
5. Olivotto M, Caldini R, Chevanne M, Cipolleschi MG. The respiration-linked limiting step of tumor cell transition from the non-cycling to the cycling state: its inhibition by oxidizable substrates and its relationships to purine metabolism. J Cell Physiol 1983; 116:149-58; PMID:6863398; http://dx.doi.org/10.1002/jcp.1041160205
6. Olivotto M, Dello Sbarba P. Environmental restrictions within tumor ecosystems select for a convergent, hypoxia-resistant phenotype of cancer stem cells. Cell Cycle 2008; 7:176-87; PMID:18256528; http://dx.doi.org/10.4161/cc.7.2.5315
7. Takahashi K, Yamanaka S. Induction of pluripotent stem cells from mouse embryonic and adult fibroblast cultures by defined factors. Cell 2006; 126:663-76; PMID:16904174; http://dx.doi.org/10.1016/j.cell.2006.07.024
8. Lozzio CB, Lozzio BB. Human chronic myelogenous leukemia cell-line with positive Philadelphia chromosome. Blood 1975; 45:321-34; PMID:163658
9. Koeffler HP, Golde DW. Human myeloid leukemia cell lines: a review. Blood 1980; 56:344-50; PMID:6996765
10. Potter VR, Reif AE. Inhibition of an electron transport component by antimycin A. J Biol Chem 1952; 194:287-97; PMID:14927618
11. Del Monte U, Olivotto M. Research on the nature of the substrates of endogenous respiration of Yoshida's ascites hepatoma. Sperimentale 1965; 115:405-22; PMID:4164352
12. Zetterberg A, Engström W. Glutamine and the regulation of DNA replication and cell multiplication in fibroblasts. J Cell Physiol 1981; 108:365-73; PMID:7287825; http://dx.doi.org/10.1002/jcp.1041080310
13. DeBerardinis RJ, Mancuso A, Daikhin E, Nissim I, Yudkoff M, Wehrli S, Thompson CB. Beyond aerobic glycolysis: transformed cells can engage in glutamine metabolism that exceeds the requirement for protein and nucleotide synthesis. Proc Natl Acad Sci U S A 2007; 104:19345-50; PMID:18032601; http://dx.doi.org/10.1073/pnas.0709747104
14. Vander Heiden MG, Cantley LC, Thompson CB. Understanding the Warburg effect: the metabolic requirements of cell proliferation. Science 2009; 324:1029-33; PMID:19460998; http://dx.doi.org/10.1126/science.1160809
15. Santini R, Vinci MC, Pandolfi S, Penachioni JY, Montagnani V, Olivito B, Gattai R, Pimpinelli N, Gerlini G, Borgognoni L, et al. Hedgehog-GLI signaling drives self-renewal and tumorigenicity of human melanoma-initiating cells. Stem Cells 2012; 30:1808-18; PMID:22730244; http://dx.doi.org/10.1002/stem.1160
16. Kaplon J, Zheng L, Meissl K, Chaneton B, Selivanov VA, Mackay G, van der Burg SH, Verdegaal EM, Cascante M, Shlomi T, et al. A key role for mitochondrial gatekeeper pyruvate dehydrogenase in oncogene-induced senescence. Nature 2013; 498:109-12; PMID:23685455; http://dx.doi.org/10.1038/nature12154
17. Maden BEH. Tetrahydrofolate and tetrahydromethanopterin compared: functionally distinct carriers in C1 metabolism. Biochem J 2000; 350:609-29; PMID:10970772; http://dx.doi.org/10.1042/0264-6021:3500609
18. Nelson DL, Cox MM. Lehninger. Principles of Biochemistry. New York: Worth Publishers Inc. 2000.
19. Cipolleschi MG, Dello Sbarba P, Olivotto M. The role of hypoxia in the maintenance of hematopoietic stem cells. Blood 1993; 82:2031-7; PMID:8104535
20. Gattei V, Bernabei PA, Ferrini PR. Differential sensitivity to (dl)-5-methyltetrahydrofolate of normal CFU-GM and HL-60 cells. Leuk Res 1989; 13:595-8; PMID:2761291; http://dx.doi.org/10.1016/0145-2126(89)90126-4
21. Bernabei PA, Mini E, Gattei V, Agostino FC, Bezzini R, Saccardi R, Santini V, Coronnello M, Mazzei T, Rossi Ferrini P. Induction of differentiation of HL-60 cells along the monocytic pathway by 5-methyltetrahydrofolate. J Chemother 1989; 1:359-64; PMID:2614501

22. Bernabei PA, Bensinger WI. Effect of (dl)-5-methyltetrahydrofolate on lymphoid leukemia cell lines. Leuk Res 1991; 15:645-9; PMID:1861546; http://dx.doi.org/10.1016/0145-2126(91)90034-Q
23. Bernabei PA, Bensinger WI. Differential effect of the combination methotrexate/(dl)-5-methyltetrahydrofolate on lymphoid malignant and normal bone marrow cells. Leukemia 1992; 6:131-5; PMID:1552744
24. Yoshida T. Gann 1934; 28:441-457.
25. Umbreit WW, Burris RH, Stauffer JF. in Manometric Techniques and Tissue Metabolism, 4a ed., Burgess Publ., Minneapolis 1964.
26. Tavazzi B, Lazzarino G, Leone P, Amorini AM, Bellia F, Janson CG, Di Pietro V, Ceccarelli L, Donzelli S, Francis JS, et al. Simultaneous high performance liquid chromatographic separation of purines, pyrimidines, N-acetylated amino acids, and dicarboxylic acids for the chemical diagnosis of inborn errors of metabolism. Clin Biochem 2005; 38:997-1008; PMID:16139832; http://dx.doi.org/10.1016/j.clinbiochem.2005.08.002
27. Giuntoli S, Rovida E, Barbetti V, Cipolleschi MG, Olivotto M, Dello Sbarba P. Hypoxia suppresses BCR/Abl and selects imatinib-insensitive progenitors within clonal CML populations. Leukemia 2006; 20:1291-3; PMID:16710305; http://dx.doi.org/10.1038/sj.leu.2404224
28. Dello Sbarba P, Cipolleschi MG, Olivotto M. Hemopoietic progenitor cells are sensitive to the cytostatic effect of pyruvate. Exp Hematol 1987; 15:137-42; PMID:3817047
29. Olivotto M, Boddi V, Dello Sbarba P, Arcangeli A. A comparative kinetic analysis of proliferation in vitro of con-A-treated splenocytes and syngeneic leukaemia cells. Cell Tissue Kinet 1982; 15:623-36; PMID:7172199